Molecular Crystals and Liquid Crystals
Publication details, including instructions for authors and subscription information:
http://www.tandfonline.com/loi/gmcl16

Chain Ordering in the Smectic C, Smectic A and Nematic Phases of Terephtal-bis-butyl-aniline (TBBA) and its Temperature Dependence

F. Volino [a] , A. J. Dianoux [b] , J. Berges [c] & H. Perrin [c]
[a] CNRS and Equips de Physico-Chimie Moléculaire, PHS, DRF, CENG, 85X, 38041, Grenoble, Cedex, France
[b] Institut Laue-Langevin, 156X, 38042, Grenoble, Cedex, France
[c] Laboratoire de Physique Moléculaire, University P. et M. Curie, Tour 22, 4, Place Jussieu, 75230, Paris, Cedex, France
Version of record first published: 20 Apr 2011.

Mol. Cryst. Liq. Cryst., 1983, Vol. 90, pp. 281–306
0026-8941/83/9004-0281$18.50/0

Printed in the United States of America

Chain Ordering in the Smectic C, Smectic A and Nematic Phases of Terephtal-bis-butyl-aniline (TBBA) and its Temperature Dependence:

A Study in Terms of Intermolecular Potentials and Changes in the Molecular Free Volume

F. VOLINO

CNRS and Equipe de Physico-Chimie Moléculaire, PHS, DRF, CENG, 85X, 38041 Grenoble Cedex, France

A. J. DIANOUX

Institut Laue-Langevin, 156X, 38042 Grenoble Cedex, France

J. BERGES and H. PERRIN

Laboratoire de Physique Moléculaire, Université P. et M. Curie, Tour 22, 4, Place Jussieu, 75230 Paris Cedex, France

(*Received July 6, 1982*)

The deuterium magnetic resonance (DMR) data of Deloche *et al.* (*J. Physique, Coll.*, **36** (1975) C1-21) on the smectic C, smectic A and nematic phases of TBBA, concerning the butyl chains, are analyzed in terms of a model where the chain ordering is described by mean rotational potentials hindering the rotations around the C—C single bonds. These potentials are split into intra and intermolecular contributions. Using intramolecular potentials calculated with quantum chemistry methods, we estimate the shapes and the heights of the intermolecular contributions. We find that (i) the intermolecular potentials favor chain conformations which are aligned with the long molecular axis, (ii) their heights decrease as the temperature (or equivalently the molar volume) increases, (iii) the most probable conformation of the chains slightly changes with temperature, but is always very different from that of the isolated molecule.

These results are additional support for the model we already proposed for the aromatic core of TBBA[14,15] and for PAA,[18] to explain the temperature dependence of DMR

splitting ratios in liquid crystals, in terms of changes of the most probable conformation (associated with changes of the free volume per molecule) rather than in terms of several, temperature dependent, molecular orientational order parameters.[5,7,8]

1. INTRODUCTION

The problem of chain ordering in liquid crystals has been the subject of considerable work in these recent years, especially because it is now possible to obtain rather accurate deuterium magnetic resonance (DMR) data of partially or fully deuterated samples. These data may be used to test molecular mean field theories of nematics which include the conformational motions of the chains[1,2] and this has been attempted in some cases.[3,4] Other theories have been developed,[5,6] based on the observed temperature dependence of DMR splitting ratios in some systems, but a number of counter examples[3,7-11] shows that they cannot be general descriptions of the liquid crystalline state. Finally, simple molecular models have been proposed, mainly based on the rotameric state model of Flory.[12] In these models, the probability of occurrence of the various rotational states of the chains is modified in order to take into account the influence of the nematic medium. These models can account for the general features of the DMR data, but cannot explain in detail the relative values of the splittings and their temperature dependence.[9,13]

In a previous paper[14] we have proposed a model to explain quantitatively the temperature dependence of DMR splitting ratios in the smectic C, smectic A and nematic phases of terephtal-bis-butyl-aniline (TBBA), these ratios being associated with the aromatic core of the molecule. In this model (i) the molecules are assumed to rotate uniformly around their long axis (ii) the rigid fragments rotate around single covalent bonds and (iii) the most probable molecular conformation changes with temperature. We obtained evidence for the uniform rotation after a detailed comparative analysis of optical, neutron, ^{14}N NQR and DMR data.[15] Evidence for the intramolecular rotations in TBBA is contained in the structure of the DMR spectra[16,17] and the fact that this phenomenon is general in liquid crystals is presently well accepted. Finally, concerning the conformational changes, we argued[14] that they correspond mainly to changes in the height and in the shape of the mean rotational potentials around the single covalent bonds, due to significant changes of the mean intermolecular forces with temperature. As temperature increases, these forces decrease due to an increase of the free volume per molecule (thermal expansion) and the

mean rotational potentials change in such a way that they tend towards those of the isolated molecule. This model was successfully applied not only to TBBA,[14] but also to nematic PAA.[18]

In this paper, we extend the analysis on the aromatic core[14] to the butyl chains of TBBA. Using the same kind of model, we estimate the mean rotational potentials, considered as the sum of intra and intermolecular contributions, hindering the rotations around the C—C single bonds of the chains. We find that (i) the height of both contributions are comparable (a few Kcal/mole) but their shapes are different, and (ii) the height of the intermolecular contributions decrease with increasing temperature, as expected from the above considerations. For all temperatures, the most probable conformation of the chain is found to differ from that of the isolated molecule. In section 2 we calculate the theoretical expressions for the splittings, associated with the deuterons of the butyl chains, in terms of chain order parameters describing the rotations around the C—C single bonds. In section 3 we discuss the nature of the potentials hindering these rotations. In section 4, we propose to replace these complex potentials by mean potentials associated with each C—C bond. This simplification is justified using theoretical results concerning the isolated molecule. In section 5 and 6, we use this approximation to analyze the DMR data in the liquid crystal phases. The shapes and heights of the intermolecular and total mean potentials are deduced and compared to those of the isolated molecule. In section 7, we discuss the physical meaning of these results, and comment on different approaches to similar data.

2. THEORETICAL EXPRESSION OF THE DMR SPLITTINGS

2.1 Definitions and notations

We follow the method of Ref. [14]. We define a molecular frame $Ox_0y_0z_0$ that we associate to the most probable molecular conformation, i.e. the conformation such that all the dihedral angles between rigid molecular fragments linked between themselves by single covalent bonds, correspond to minima of the rotational potentials around these bonds. This molecular frame is assumed to rotate uniformly around its long axis Oz_0. Then, we associate a frame $Ox_my_mz_m$, with Oz_m along the internal rotation axis, to each "most probable fragment". The long axis is defined by a set of polar and azimuthal angles $\{\epsilon, \phi\}$ in these most probable frames. Finally, we attach a frame $Oxyz$ with $Oz \equiv Oz_m$ to each fragment, which is used to describe the rotation of this fragment with respect to a frame attached to the most probable molecule, e.g.

(but not necessarily) the $Ox_my_mz_m$ frame.

Since each fragment of the TBBA molecule has at least one C_{1v} symmetry plane containing Oz (no chiral group exists in TBBA), we choose Ox in this plane. For the i^{th} methylene group of the chains, Oz_i is along the $\mathbf{C}_{i-1}\mathbf{C}_i$ bond and Ox_i in the bissector plane of the two C_iD bonds. This plane also contains the C_iC_{i+1} bond. The orientation of Ox_i is chosen such that the x components of the two $\mathbf{C}_i\mathbf{D}$ vectors are negative (and consequently, the x component of $\mathbf{C}_i\mathbf{C}_{i+1}$ is positive). The polar and azimuthal angles of the two $\mathbf{C}_i\mathbf{D}$ vectors are u_D, φ_D and u_D, $-\varphi_D$; those of the $\mathbf{C}_i\mathbf{C}_{i+1}$ vector are u_c, 0. With these conventions, we have $u_c < 90°$, $u_D < 90°$, $\varphi_D > 90°$. Figure 1 summarizes these definitions. It should be noticed that u_c, u_D and φ_D are not independent angles since the C_iD bonds make the same angle with the two adjacent C_iC_{i-1} and C_iC_{i+1} bonds. Simple geometrical considerations show that we have

$$\cos \varphi_D = -\frac{1 + \cos u_c}{\sin u_c \tan u_D} \tag{1}$$

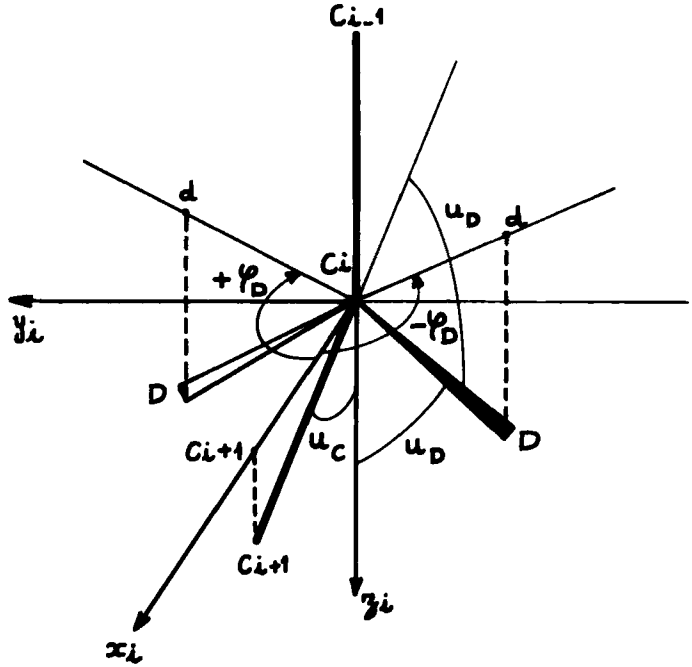

FIGURE 1 Geometry of the methylene group associated with carbon C_i of an aliphatic chain. Oz_i is chosen along $C_{i-1}C_i$ and Ox_i is such that the x component of the C_iC_{i+1} vector is positive. The various angles defined in the text are shown.

To describe the rotations around the C—C bonds of the chains, we define the following frames, as indicated in Figure (2): (i) the frame $Ox^{er}y^{er}z^{er}$ is attached to the most probable orientation of the *phenyl ring* and, in this frame, the polar and azimuthal angles of the long axis Oz_0 are called ϵ, ϕ, without indexes for simplicity; (ii) the $C_1x_1y_1z_1$ frame with $C_1z_1 \equiv Oz^{er}$, is attached to the first methylene group and is used to describe the rotation of this group in the $Ox^{er}y^{er}z^{er}$ frame, the corresponding rotation angle being $\varphi_1 = (C_1x^{er}, C_1x_1)$; (iii) the frame $C_2x_2y_2z_2$ is attached to the second methylene group and is used to describe the rotation of this group in the $C_2x_1^0y_2^0z_2^0$ frame with $C_2z_2^0 \equiv C_2z_2$, the corresponding rotation angle being $\varphi_2 = (C_2x_2^0, C_2x_2)$. This $C_2x_2^0y_2^0z_2^0$ frame is attached to the $C_BC_1C_2$ plane and is oriented as indicated on Figure 2, namely such that the trans conformation corresponds to $\varphi_2 = 180°$; (iv) similarly we define $C_3x_3y_3z_3$, $C_3x_3^0y_3^0z_3^0$, $\varphi_3 = (C_3x_3^0, C_3x_3)$ for the third methylene group, and so on for the following groups. With these definitions, the all-trans, planar, conformation corresponds to $\varphi_i = 180°(i > 1)$, as drawn on Figure 2 for a butyl chain.

2.2 Expressions for the DMR splittings associated with the butyl chains. Following Ref. [14], assuming that (i) the e.f.g. tensor acting on one deuteron D_i has cylindrical symmetry around the CD_i bond (ii) the molecular frame rotates uniformly around its long axis Oz_0 and (iii) the

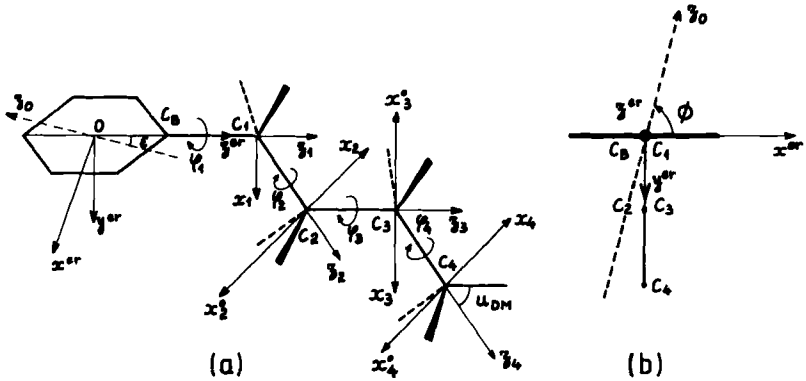

FIGURE 2 Sketch of the butyl-benzene group of TBBA, in its most probable conformation for the isolated molecule, showing the various angles and frames defined in the text. The plane of the ring is perpendicular to the all-trans plane. a) lateral view, b) top view along the para-axis of the ring. The polar and azimuthal angles ϵ, ϕ of the long molecular axis Oz_0 in the $Ox^{er}y^{er}z^{er}$ frame associated with the ring, are also indicated. The origin of the rotation angles around C_1C_2, C_2C_3, C_3C_4 being x_2^0, x_3^0, x_4^0 respectively, the all-trans conformation corresponds to $\varphi_2 = \varphi_3 = \varphi_4 = 180°$.

external and internal motions are not coupled, and fast on the DMR time scale ($\sim 10^{-6}$ s), then the DMR splitting $\Delta\nu_i$ associated with any deuteron D_i is given by

$$\Delta\nu_i = \frac{3}{2} c_i S \langle P_2[\cos(Oz_0, CD_i)]\rangle \tag{2}$$

where $c_i = e^2 q_i Q/h$ is the quadrupolar coupling constant, $S \equiv S_{z_0z_0}$ is the usual nematic order parameter and the brackets stand for an averaging over the internal motions. Expressing the P_2 in the $Ox^{er}y^{er}z^{er}$ frame, we can write

$$P_2[\cos(Oz_0, CD_i)] = \frac{4\pi}{5} \sum_{m=-2}^{+2} Y_2^{m*}(\epsilon, \phi) Y_2^m(\Omega_i^{er}) \tag{3}$$

where Ω_i^{er} symbolizes the polar and azimuthal angles of CD_i in the $Ox^{er}y^{er}z^{er}$ frame.

The problem reduces in evaluating $Y_2^m(\Omega_i^{er})$ for the successive methylene groups and performing the average. For the calculation, we use the following two well known identities

$$Y_l^m(\beta, \alpha) = \left(\frac{2l+1}{4\pi}\right)^{1/2} d_{m0}^l(\beta) e^{im\alpha} \tag{4}$$

$$D_{mm'}^l(\alpha, \beta, \gamma) = e^{-im\alpha} d_{mm'}^l(\beta) e^{im'\gamma} \tag{5}$$

where the $D_{mm'}^l$ and $d_{mm'}^l$ are the normal and reduced Wigner matrices of order l, respectively.[19]

(*a*) *First methylene group* In the $C_1x_1y_1z_1$ frame, the polar and azimuthal angles of C_1D are u_D, $\pm\varphi_D$; in the $Ox^{er}y^{er}z^{er}$ frame, they are u_D, $\pm\varphi_D + \varphi_1$, so that

$$Y_2^{m_1}(\Omega_1^{er}) = Y_2^{m_1}(u_D, \pm\varphi_D + \varphi_1) \tag{6}$$

Using Eq. (4), we obtain

$$P_2[\cos(Oz_0, C_1D)] = \sum_{m_1=-2}^{2} d_{m_10}^2(\epsilon) d_{m_10}^2(u_D) e^{i(-m_1\phi \pm m_1\varphi_D)} e^{im_1\varphi_1} \tag{7}$$

(*b*) *Second methylene group* In the $C_2x_2^0y_2^0z_2^0$ frame, the polar and azimuthal angles of C_2D are u_D and $\pm\varphi_D + \varphi_2$. To bring this frame on to the $Ox^{er}y^{er}z^{er}$ frame, we perform the rotation with Euler angles $-\varphi_1$,

u_c, π. We thus have

$$Y_2^{m_1}(\Omega_2^{er}) = \sum_{m_2=-2}^{2} D^2_{m_1 m_2}(-\varphi_1, u_c, \pi) Y_2^{m_2}(u_D, \pm\varphi_D + \varphi_2) \tag{8}$$

Using Eqs. (4) and (5), we obtain

$$P_2[\cos(Oz_0, C_2D)] = \sum_{m_1, m_2} e^{im_2\pi} d^2_{m_1 0}(\epsilon) d^2_{m_1 m_2}(u_c) d^2_{m_2 0}(u_D) e^{i(-m_1\phi \pm m_2\varphi_D)} e^{i(m_1\varphi_1 + m_2\varphi_2)} \tag{9}$$

(*c*) *Third methylene group* Similarly, in the $C_3x_3^0y_3^0z_3^0$ frame, the polar and azimuthal angles of C_3D are u_D, $\pm\varphi_D + \varphi_3$. To bring the $C_3x_3^0y_3^0z_3^0$ frame on to the $Ox^{er}y^{er}z^{er}$ frame, we perform two successive rotations of Euler angles $-\varphi_2$, $-u_c$, π and $-\varphi_1$, $+u_c$, π. This yields:

$$Y_2^{m_1}(\Omega_3^{er}) = \sum_{m_2 m_2} D^2_{m_1 m_2}(-\varphi_1, u_c, \pi) D^2_{m_2 m_3}(-\varphi_2, -u_c, \pi) Y_2^{m_3}(u_D, \pm\varphi_D + \varphi_3) \tag{10}$$

Using Eq. (4) and (5), we obtain

$$P_2[\cos(Oz_0, C_3D)] = \sum_{m_1, m_2, m_3} e^{i(m_2+m_3)\pi} d^2_{m_1 0}(\epsilon) d^2_{m_1 m_2}(u_c) d^2_{m_2 m_3}(-u_c) d^2_{m_3 0}(u_D) e^{i(-m_1\phi \pm m_3\varphi_D)} \times e^{i(m_1\varphi_1 + m_2\varphi_2 + m_3\varphi_3)} \tag{11}$$

(*d*) *Fourth group* Similarly we find

$$P_2[\cos(Oz_0, C_4D)] = \sum_{m_1, m_2, m_3, m_4} e^{i(m_2+m_3+m_4)\pi} d^2_{m_1 0}(\epsilon) d^2_{m_1 m_2}(u_c) d^2_{m_2 m_3}(-u_c) d^2_{m_3 m_4}(u_c) d^2_{m_4 0}(u_D) e^{i(-m_1\phi \pm m_4\varphi_D)} \times e^{i(m_1\varphi_1 + m_2\varphi_2 + m_3\varphi_3 + m_4\varphi_4)} \tag{12}$$

The expression is easily generalized for the i^{th} group of an alkyl chain of any length. Note the alternation $+u_c$, $-u_c$, $+u_c$ . . . for the arguments of the successive d^2.

To obtain the expression of the splittings, we should average the above expressions over the internal motions. These internal motions are of two kinds: rotation around the chain C—C bonds and exchange between, equivalent, most probable conformations.

(i) the average over the rotations around the C—C bonds are governed by the potential

$$V\{\varphi_i\} = V(\varphi_1, \varphi_2, \varphi_3, \varphi_4) \tag{13}$$

according to the Boltzmann law:

$$\langle f\{\varphi_i\}\rangle = Z^{-1}\int d\{\varphi_i\} f\{\varphi_i\} e^{-V\{\varphi_i\}/k_BT} \tag{14}$$

where f is any function of the φ_i, and Z a normalization constant

$$Z = \int d\{\varphi_i\} e^{-V\{\varphi_i\}/k_BT} \tag{15}$$

Since the all-trans conformation is a symmetry plane of the chain, the potential $V\{\varphi_i\}$ is necessarily symmetric i.e. $V\{-\varphi_i\} = V\{\varphi_i\}$. This implies that the averages of the exponentials containing the φ_i in Eqs. (7,9,11,12) reduce to the average of their cosine.

(ii) the most probable conformations defined by the two sets $\{\epsilon, \phi\}$ and $\{\epsilon, -\phi\}$ are energetically equivalent since no asymmetrical group exists in TBBA. If they exchange rapidly on the DMR time scale, one should average further Eqs. (7,9,11,12) over $\pm\phi$.

Performing these two averages independently and using the symmetry relation of the d^2,[19] it can be shown that the four splittings of the butyl chains are finally given by:

$$\Delta\nu_1 = \frac{3}{2} c_1 S \sum_{m_1} d^2_{m_1 0}(\epsilon) d^2_{m_1 0}(u_D) \cos m_1\phi \cos m_1\varphi_D \langle \cos m_1\varphi_1\rangle \tag{16}$$

$$\Delta\nu_2 = \frac{3}{2} c_2 S \sum_{m_1 m_2} (-1)^{m_2} d^2_{m_1 0}(\epsilon) d^2_{m_1 m_2}(u_c) d^2_{m_2 0}(u_D) \times \cos m_1\phi \cos m_2\varphi_D \langle \cos m_1\varphi_1 \cos m_2\varphi_2\rangle \tag{17}$$

$$\Delta\nu_3 = \frac{3}{2} c_3 S \sum_{m_1 m_2 m_3} (-1)^{m_2+m_3} d^2_{m_1 0}(\epsilon) d^2_{m_1 m_2}(u_c) d^2_{m_2 m_3}(-u_c) d^2_{m_3 0}(u_D) \times \cos m_1\phi \cos m_3\varphi_D \langle \cos m_1\varphi_1 \cos m_2\varphi_2 \cos m_3\varphi_3\rangle \tag{18}$$

$$\Delta\nu_4 = \frac{3}{2} c_4 S \sum_{m_1 m_2 m_3} (-1)^{m_2+m_3} d^2_{m_1 0}(\epsilon) d^2_{m_1 m_2}(u_c) d^2_{m_2 m_3}(-u_c) d^2_{m_3 0}(u_c) d_{00}(u_{DM}) \times \cos m_1\phi \langle \cos m_1\varphi_1 \cos m_2\varphi_2 \cos m_3\varphi_3\rangle \tag{19}$$

For the methyl splitting $\Delta\nu_4$, we have further assumed that the methyl rotation is not coupled with the other rotations and has C_{3v} symmetry, i.e. $\langle \cos \varphi_4\rangle = \langle \cos 2\varphi_4\rangle = 0$. This reduces the sum over three indices

instead of four. The corresponding u_D angle is assumed to be slightly different than for the methylene groups: u_{DM}.

These equations show in particular that the splittings are the same for $\pm\varphi_D$, i.e. that the two deuterons of the same methylene group are magnetically equivalent. This equivalence comes from the symmetry of the potential $V\{\varphi_i\}$ and from the average over $\pm\phi$. If the two conformations were not exactly energetically equivalent (as for example in a chiral molecule), then these two deuterons would generally not be equivalent (see also the discussion in Ref. [14]).[20]

2.3 Discussion and experimental data

It is seen that Eqs. (16–19) contain three kinds of quantities (i) the structural quantities, c_i, u_c, u_D, u_{DM}, φ_D which are expected to be practically temperature independent, and known with sufficient accuracy (ii) the conformational quantities ϵ and ϕ which can vary with temperature. In TBBA, we have shown[14] that ϵ is practically constant $\approx 7.9°$ and that ϕ varies with temperature. The variation of ϕ (which should be identified to $\phi_{c.r.} + \alpha$ of Ref. [14]) deduced from the analysis of Ref. [14] is shown in Figure 3. (iii) finally the dynamical quantities S and $p_{m_1m_2m_3}$ defined as

$$p_{m_1m_2m_3} = \langle \cos m_1\varphi_1 \cos m_2\varphi_2 \cos m_3\varphi_3 \rangle \tag{20}$$

which also are temperature dependent (except $p_{000} = 1$).

The information on the chain ordering is contained in the $3^3 = 27 p_{m_1m_2m_3}$ quantities, which can be considered as chain rotational order parameters. For each temperature, the experiment[4] yields the

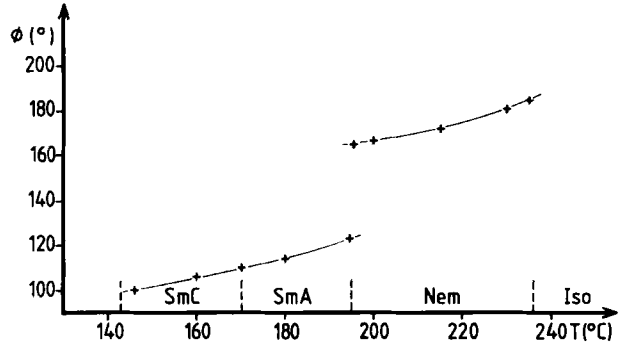

FIGURE 3 Temperature variation of the azimuthal angle ϕ of the long molecular axis Oz_0, in the $Ox^{er}y^{er}z^{er}$ frame. It has been deduced combining Figures 2, 3 and 4 of Ref. [14]. ϕ should be identified to $\phi_{c.r.} + \alpha$ of that reference.

moduli of the four DMR splittings $|\Delta\nu_i|$ (Figure 4). In order to eliminate the external parameter S, which was studied in detail in Ref. [15], we form the three ratios $|R_{i1}| = |\Delta\nu_i/\Delta\nu_1|$. These ratios are shown in Figure 5a,b for the smectic C, smectic A and nematic phases. They have been calculated using the published data.[4,21] It is seen that the $|R_{i1}|$ decrease with temperature, with discontinuities at the SmA–nematic transition. A discontinuity was also found for ϕ (cf. Figure 3). Since there are only three independent data to determine the 26 unknown $p_{m_1m_2m_3}$, it is necessary to make some assumptions on these quantities, i.e. on the rotational potential $V\{\varphi_i\}$ before any analysis can be made.

3. MODEL FOR THE POTENTIAL $V\{\varphi_i\}$.

Assuming that $V\{\varphi_i\}$ is known, we can always associate mean average potentials $\bar{V}(\varphi_i)$ to each $C_{i-1}C_i$ bond defined by

$$\bar{V}(\varphi_i) = -k_BT \,\mathrm{Ln} \iint d\varphi_j d\varphi_k e^{-V\{\varphi_i\}/k_BT} \tag{21}$$

and individual "order parameters" $p_n^{(i)}$ such that

$$p_n^{(i)} = \langle \cos n\varphi_i \rangle = Z'^{-1} \int d\varphi_i \cos n\varphi_i e^{-\bar{V}(\varphi_i)/k_BT} \tag{22}$$

The simplification we propose is to assume that, in Eqs. (16–19) we can

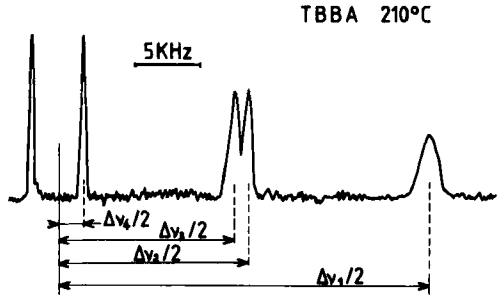

FIGURE 4 Example of DMR spectrum of TBBA deuterated on the butyl-chains in the nematic phase (extracted from Ref. 16), showing the definition of the various splittings. The assignment of $\Delta\nu_2$ to the second methylene group, starting from the ring, and $\Delta\nu_3$ to the third one, has been obtained from the analysis presented in this paper. Only half of the spectrum is shown.

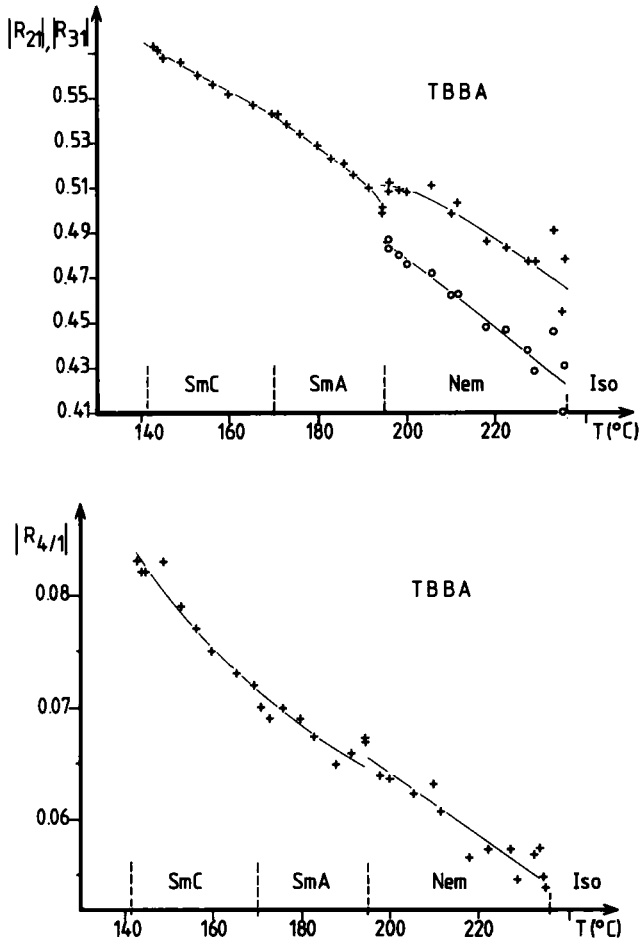

FIGURE 5 Temperature variation of the ratios $|R_{i1}|$ for the chains of TBBA deduced from Ref. (4). a) $|R_{21}| = |\Delta\nu_2/\Delta\nu_1|$ and $|R_{31}| = |\Delta\nu_3/\Delta\nu_1|$. The assignment is such that $|R_{21}| > |R_{31}|$ in the nematic phase, as deduced from the analysis presented in this paper. b) $|R_{41}| = |\Delta\nu_4/\Delta\nu_1|$. The lines are smooth curves drawn through the experimental points. The values in these lines have been used as "experimental" values for each temperature.

separate the averages over φ_1, φ_2, φ_3, i.e. that we have

$$p_{m_1m_2m_3} \approx p^{(1)}_{m_1} p^{(2)}_{m_2} p^{(3)}_{m_3} \tag{23}$$

i.e. that the real chain motion is satisfactorily described by individual rotations around the C—C bonds in the mean potentials $\bar{V}(\varphi_i)$. This assumption reduces the number of unknown parameters from 26 to 6. Since, moreover $\bar{V}(\varphi_1)$ has necessarily the C_{2v} symmetry imposed by the ring, $\langle \cos \varphi_1 \rangle = 0$ so that only five unknown quantities are left, namely $\langle \cos 2\varphi_1 \rangle$, $\langle \cos \varphi_2 \rangle$, $\langle \cos 2\varphi_2 \rangle$, $\langle \cos \varphi_3 \rangle$ and $\langle \cos 2\varphi_3 \rangle$. In this manner, the problem is considerably simplified and it is hoped that some useful information on these potentials can be extracted from the data.

However, before going on with the analysis, we should check in some way if the assumption Eq. (23) is reasonable. For this purpose, we write the total potential V as:

$$V\{\varphi_i\} = V_{in}\{\varphi_i\} + V_{ex}\{\varphi_i\} \tag{24}$$

where V_{in} and V_{ex} are the intramolecular (i.e. due to the electronic distribution in the molecule) and intermolecular (i.e. due to the liquid crystalline medium) contributions. In these conditions, we can define mean intra and intermolecular potentials $\bar{V}_{in}$ and $\bar{V}_{ex}$ such that:

$$\bar{V}(\varphi_i) = \bar{V}_{in}(\varphi_i) + \bar{V}_{ex}(\varphi_i) \tag{25}$$

In what follows, we use the fact that $V_{in}\{\varphi_i\}$ is known[22,23] to calculate the $\bar{V}_{in}(\varphi_i)$, and test the decoupling model for an isolated butyl chain.

4. THE ISOLATED BUTYL CHAIN: CALCULATION OF THE $\bar{V}_{in}(\varphi_i)$ AND TEST OF THE DECOUPLING HYPOTHESIS

The full potential $V_{in}\{\varphi_i\} = V_{in}(\varphi_1, \varphi_2, \varphi_3)$ for the butyl-benzene molecule, averaged over methyl rotation, has been calculated by two of us by quantum chemistry methods and the results are described in detail elsewhere.[22,23] Using this potential, we have calculated the $\bar{V}_{in}(\varphi_i)$ defined by Eq. (21) where V is replaced by V_{in}, by numerical integration by steps of 15°. The results are shown in Figure 6a,b,c for $\bar{V}_{in}(\varphi_1)$, $\bar{V}_{in}(\varphi_2)$, $\bar{V}_{in}(\varphi_3)$, for two extreme temperatures of the DMR experiment, namely 146°C and 230°C. For convenience, in these figures and other similar ones later on, the origin of energies has been chosen such that the constant term in the Fourier expansion is zero. The first point to be noticed is that their height is comparable (3 to 4 Kcal/mole) and extremely weakly temperature dependent in this range. Concerning their shape, $\bar{V}_{in}(\varphi_1)$ varies practically as $\cos 2\varphi_1$, with minima at $\varphi_1 = 90°$ and 270°.

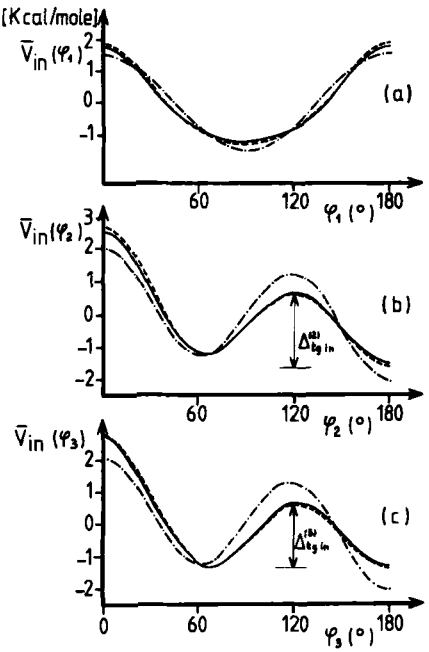

FIGURE 6 Shape of the mean intramolecular potentials for the butyl-benzene molecule defined by Eq. (21) for the two extreme temperatures: ——: 146°C; – – – –: 230°C. a) $\bar{V}_{in}(\varphi_1)$; a pure cos $2\varphi_1$ shape is also shown; b) $\bar{V}_{in}(\varphi_2)$; c) $\bar{V}_{in}(\varphi_3)$. The butane potential[25] is also shown: —·—·— in b) and c) for comparison.

This means that for the isolated molecule, the most probable orientation of the plane of the all-trans chain is perpendicular to the plane of the ring, as in the solid phase.[24] Concerning $\bar{V}_{in}(\varphi_2)$ and $\bar{V}_{in}(\varphi_3)$, their shapes are very similar with three minima at $\varphi = 180°$ (the trans position) and $\varphi \approx \pm 60°$ (the gauche positions). For comparison we have drawn the well known butane-potential[25] which has been found for the butane molecule. It is seen that the shape is similar, with minima at about the same places, but the details are different. In particular, the difference between the trans and gauche positions is ≈0.7 Kcal/mole for the butane, but only ≈0.25 for $\bar{V}_{in}(\varphi_2)$ and practically zero for $\bar{V}_{in}(\varphi_3)$. Moreover, the barrier height between these two positions is higher for the butane molecule. This means that the isolated butyl chain is more disordered than the isolated butane molecule, since all-trans or trans-gauche conformations have practically the same energy.

Using these average potentials, that we have simulated by their Fourier expansion until the sixth term, we have calculated the chain order parameters $p_n^{(i)}$ defined by Eq. (22). Table I gives the values of the

$p^{(1)}_{m_1}p^{(2)}_{m_2}p^{(3)}_{m_3}$ quantities for 146 and 230°C. The values for any temperature can be obtained by linear interpolation. On the other hand, using the full potential $V_{in}(\varphi_1, \varphi_2, \varphi_3)$ we have calculated the $p_{m_1m_2m_3}$ defined by Eq. (20) and the results are given in Table II for the same temperatures. Comparison between Tables I and II provides a test for the decoupling hypothesis (Eq. 23). It is seen that if two indexes are zero, then the results are identical, as expected. For $m_1 = 1$, all the terms are practically zero in both Tables. In fact, they should be strictly zero by symmetry, the differences being due to the precision of the numerical calculations. It is seen that this precision is always (much) better than 0.01. Concerning the other terms, it is seen that decoupling the φ_1 motion to φ_2 and φ_3 motions is always a good approximation.

Finally, it appears that only the decoupling of φ_2 and φ_3 motions is a bad approximation. However, in this case, we observe that the corresponding numbers are comparatively very small. Consequently, we expect that their contributions to the values of the DMR splittings given by Eqs. (16) to (19) (and consequently to the ratios R_{i1}) is small, and that both models should yield practically the same values. We have checked this result by calculating the R_{i1} at 146°C for both models, using either Table I or Table II, and the following (standard) values of structural parameters: $c_1 = c_2 = c_3 = c_4 =$ (172KHz),[14] $u_c = 68°$ (corresponding to $\widehat{CCC} = 112°$),[26] $u_D = 69.8°$ (corresponding to $\widehat{CCH} = 110.2°$),[26] $\varphi_D = 123.7°$ (deduced from Eq. (1), $u_{DM} = 70.6°$ (the tetrahedral angle), $\epsilon = 7.9°$,[14] $\phi = 100°$ (Figure 3). The results are as follows:

$R_{21} = -0.3790$ $R_{31} = 0.1876$ $R_{41} = -0.0350$ with Table I and
$R_{21} = -0.3793$ $R_{31} = 0.1727$ $R_{41} = -0.0433$ with Table II

It is seen that the differences between the two sets of values namely ≈0.003, 0.015 and 0.0083, respectively, are very small compared with the differences with the experimental values (Figure 5a,b), namely ~0.2, 0.4 and 0.1. This shows that the uncoupled model will be sufficient to describe satisfactorily the differences in ordering between the isolated chains and the chains in the liquid crystalline medium. We shall thus use this model in the following sections.

5. THE BUTYL CHAIN IN THE LIQUID CRYSTAL: ANALYSIS IN TERMS OF CHAIN ORDER PARAMETERS.

The aim of this section is to use the above results and the experimental values of $|R_{21}|$, $|R_{31}|$ and $|R_{41}|$ to deduce information on the chain order parameters in the liquid crystal phases of TBBA.

TABLE I

$p^{(1)}_{m_1} p^{(2)}_{m_2} p^{(3)}_{m_3}$

	m_2, m_3 / m_1	0,0	0,1	0,2	1,0	1,1	1,2	2,0	2,1	2,2
146°C	0	1.000	−0.116	−0.147	−0.216	0.025	0.032	0.020	−0.002	−0.029
	1	−0.008	0.001	0.001	0.002	0.000	0.000	0.000	0.000	0.000
	2	−0.585	0.068	0.086	0.126	−0.015	−0.086	−0.012	−0.001	−0.002
230°C	0	1.000	−0.132	−0.135	−0.231	0.030	0.031	0.018	−0.002	−0.002
	1	−0.010	0.001	0.001	0.002	0.000	−0.000	−0.000	0.000	0.000
	2	−0.541	0.071	0.073	0.125	−0.016	−0.017	−0.010	−0.001	−0.001

TABLE II

$p_{m_1 m_2 m_3}$

	m_2, m_3 / m_1	0,0	0,1	0,2	1,0	1,1	1,2	2,0	2,1	2,2
146°C	0	1.000	−0.116	−0.147	−0.216	−0.050	0.062	0.020	0.057	−0.016
	1	−0.008	0.001	0.001	0.004	0.000	−0.001	−0.002	−0.001	0.001
	2	−0.585	0.084	0.087	0.103	0.037	−0.032	0.020	−0.040	0.002
230°C	0	1.000	−0.132	−0.135	−0.231	−0.045	0.056	0.018	0.054	−0.011
	1	−0.010	0.001	0.001	0.005	0.000	−0.001	−0.002	−0.001	0.001
	2	−0.541	0.089	0.075	0.096	0.033	−0.026	0.021	−0.034	0.002

As stated above, in the framework of the uncoupled model, these parameters are the five temperature dependent quantities $\langle\cos 2\varphi_1\rangle$, $\langle\cos \varphi_2\rangle$, $\langle\cos 2\varphi_2\rangle$, $\langle\cos \varphi_3\rangle$, $\langle\cos 2\varphi_3\rangle$ which appear in the expression of the splittings Eqs. (16–19). The experiment yields three independent data only, viz the $|R_{i1}|$. In practice however, the number of unknown parameters is only four since we can fix $\langle\cos 2\varphi_1\rangle$ to about -0.7. The argument is that since for the isolated molecule, and for the solid, the minimum of $\bar{V}(\varphi_1)$ is 90°, we can reasonably assume that this situation persists in the liquid crystal, the only effect of the medium to increase the height $\Delta\bar{V}^{(1)}$ of this potential. For the isolated molecule $\Delta\bar{V}^{(1)}_{in} \approx 3$ Kcal/mole corresponding to $\langle\cos 2\varphi_1\rangle \approx -0.59$. With $\overline{\Delta V}^{(1)} \approx 6$ Kcal/mole the result is $\langle\cos 2\varphi_1\rangle \approx -0.7$. In fact, we have verified that the values of the $|R_{i1}|$ are practically constant for $\langle\cos 2\varphi_1\rangle$ varying from -0.59 to -0.7. Consequently, we have fixed $\langle\cos 2\varphi_1\rangle$ to -0.7 for simplicity, and we are left with four parameters, namely $\langle\cos \varphi_2\rangle$, $\langle\cos 2\varphi_2\rangle$, $\langle\cos \varphi_3\rangle$, $\langle\cos 2\varphi_3\rangle$, to be determined with three data. For each temperature, we can thus calculate three of these parameters as a function of the fourth one, by solving numerically the corresponding set of nonlinear equations.

In fact, the situation is not so simple since the R_{i1} are *algebraical* quantities while the experiment yields only absolute values. In the present case, there are a priori $2^3 = 8$ possibilities for the combination of the three signs, so that some physics should be invoked to choose between them. The condition we impose is that the potential $\bar{V}(\varphi_2)$ should be such that the trans-position is more favored in the liquid crystal than for the isolated molecule, or in other words, that in average, the medium forces the chains to be more aligned with the long molecular axis. In terms of order parameters, this means that $\langle\cos \varphi_2\rangle$ should be between -0.23 (the isolated chain) and -1 (the rotation quenched at $\varphi_2 = 180°$). Although we can find solutions for several combinations of signs, only the combinations [-,+,+] and [−,+,−] give results which satisfy the above condition. Figure 7 shows the values of $\langle\cos \varphi_2\rangle$, $\langle\cos 2\varphi_2\rangle$ and $\langle\cos 2\varphi_3\rangle$ versus $\langle\cos \varphi_3\rangle$ for the two above combinations of signs, at 146°C, taking as experimental values of the $|R_{i1}|$ those deduced by drawing a smooth curve through the points in Figure (4a,b). An interesting feature is that for both cases, $\langle\cos \varphi_2\rangle$ and $\langle\cos 2\varphi_2\rangle$ are practically independent of $\langle\cos \varphi_3\rangle$ so that their values are practically determined. The results are similar for all temperatures. Without any further assumption or modelization, the final result of the analysis would be, for each temperature, two possible values for the set $\{\langle\cos \varphi_2\rangle, \langle\cos 2\varphi_2\rangle\}$ and two associated possible relationships between

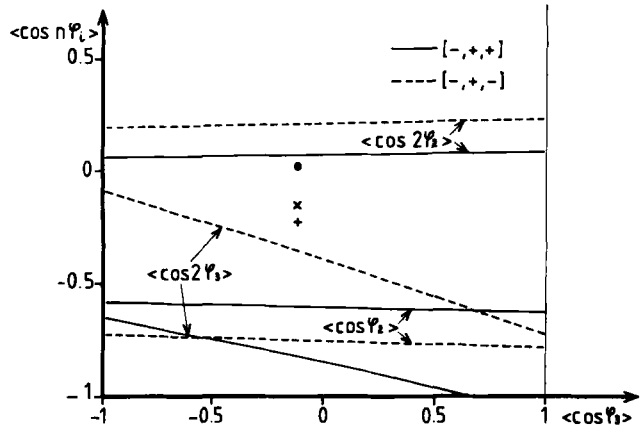

FIGURE 7 Possible values of $\langle\cos\varphi_2\rangle$, $\langle\cos 2\varphi_2\rangle$, $\langle\cos 2\varphi_3\rangle$ versus $\langle\cos\varphi_3\rangle$ corresponding to the experimental values of the $|R_{i1}|$ at 146°C, for the two possible combinations of signs of R_{21}, R_{31}, R_{41}: [−,+,+] and [−,+,−]. The values for the isolated chain are also shown. +: $\langle\cos\varphi_2\rangle_{in}$; ⊙: $\langle\cos 2\varphi_2\rangle_{in}$; ×: $\langle\cos 2\varphi_3\rangle_{in}$. See section 5 for details.

$\langle\cos\varphi_3\rangle$ and $\langle\cos 2\varphi_3\rangle$. Although this is certainly a valuable information, it is difficult to visualize their signification and remove the uncertainty. In the next section, we shall use the fact that the $\bar{V}_{in}$ are known to repeat the analysis in terms of the intermolecular potentials $\bar{V}_{ex}$. These potentials are indeed very direct information about the liquid crystal medium.

6. THE BUTYL CHAIN IN THE LIQUID CRYSTAL: ANALYSIS IN TERMS OF MEAN INTERMOLECULAR POTENTIALS.

Combining Eqs. (16 to 19, 22 and 25), it is seen that the only unknown quantities in the expression of the R_{i1} are those which define $\bar{V}_{ex}(\varphi_2)$ and $\bar{V}_{ex}(\varphi_3)$. In order to work with four unknown parameters as above, we have assumed that we have

$$\bar{V}_{ex}(\varphi_2) = a_2 \cos\varphi_2 + b_2 \cos 2\varphi_2 \tag{26}$$

and

$$\bar{V}_{ex}(\varphi_3) = a_3 \cos\varphi_3 + b_3 \cos 2\varphi_3 \tag{27}$$

i.e. that these two potentials are satisfactorily represented by the two first terms of their Fourier expansion. Fixing $\langle\cos 2\varphi_1\rangle = -0.7$ as in

the preceding section and choosing ϕ as given by Figure 3, the four unknown parameters are now a_2, b_2, a_3, b_3 to be determined by the three experimental $|R_{il}|$. As above, by solving numerically a set of 3 nonlinear equations, we can calculate three of these parameters as a function of the fourth one.

6a. The smectic C and A phases

We have first considered the SmC and SmA phases where $|\Delta\nu_2| = |\Delta\nu_3|$ so that there is no ambiguity concerning the assignment of the corresponding lines. Concerning the two possible combinations of signs of the R_{il}, after a few tentative fits, it turned rapidly out that only the combination [−,+,+] gives reasonable results, as will be explained below, so that we detail now the results of this combination of signs only.

It is found that for this combination of signs, solutions exist, where the amplitudes a_2, b_2, a_3, b_3 are such that $\bar{V}_{ex}(\varphi_2)$ and $\bar{V}_{ex}(\varphi_3)$ are maximum at $\varphi = 0$ and 180° and minimum in between at $\varphi_{2min} = \cos^{-1}(-a_2/4b_2)$ and $\varphi_{3min} = \cos^{-1}(-a_3/4b_3)$. Instead of presenting the results in terms of the a and b parameters, we can equivalently use the more physical quantities φ_{2min}, φ_{3min}, $\Delta\bar{V}_{ex}^{(2)}$ and $\Delta\bar{V}_{ex}^{(3)}$ where these $\Delta\bar{V}$ are the full heights of $\bar{V}_{ex}(\varphi_2)$ and $\bar{V}_{ex}(\varphi_3)$ respectively. For convenience, we have represented the results as $\Delta\bar{V}_{ex}^{(2)}$, $\Delta\bar{V}_{ex}^{(3)}$ and φ_{2min} versus φ_{3min}. These results are shown in Figures 8a,b,c, respectively. They call for the following comments:

(i) solutions are found for $80° \lesssim \varphi_{3min} \lesssim 105°$, where the $\Delta\bar{V}$ are not too large.

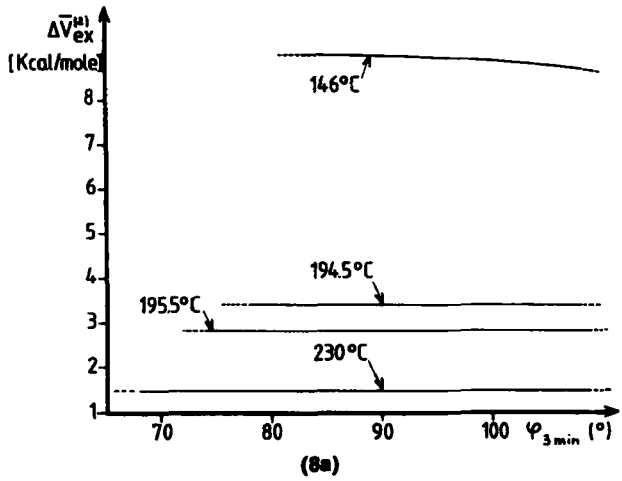

(8a)

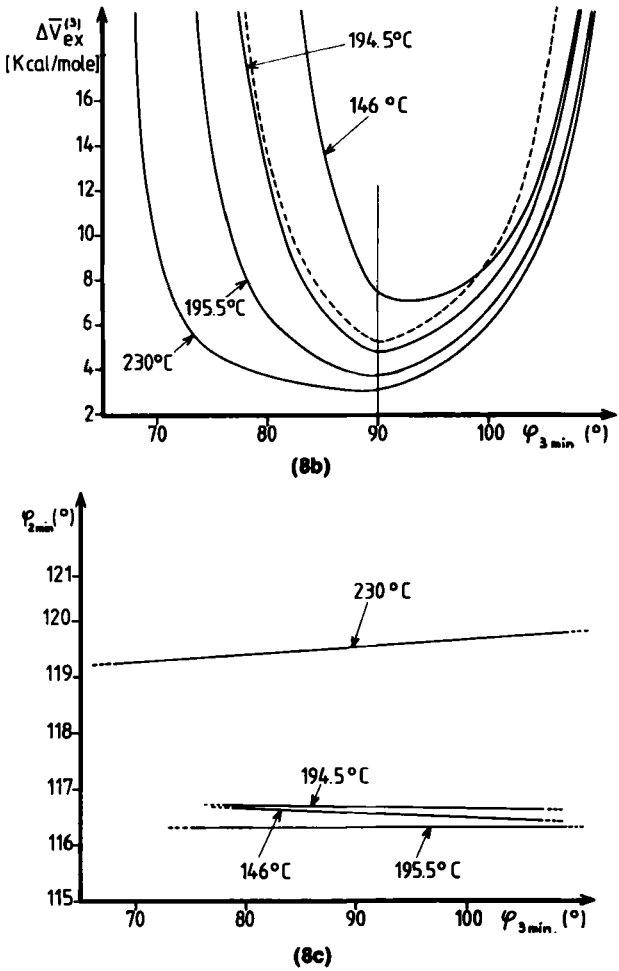

FIGURE 8 Variation of $\Delta\bar{V}_{ex}^{(2)}$, $\Delta\bar{V}_{ex}^{(3)}$ and φ_{2min} versus φ_{3min} corresponding to the experimental values of the $|R_{i1}|$, for various temperatures. The combination of signs of the R_{i1} is [−,+,+] and the assignment of the lines is such as $|R_{21}| > |R_{31}|$ in the nematic phase. a) $\Delta\bar{V}_{ex}^{(2)}$; the broken lines correspond to values of $\Delta\bar{V}_{ex}^{(3)}$ larger than 20 Kcal/mole. b) $\Delta\bar{V}_{ex}^{(3)}$; the dashed curve corresponds to 195.5°C, with the assignment $|R_{21}| < |R_{31}|$. c) φ_{2min}; idem as a) for the broken lines. See section 6 for details.

(ii) $\Delta\bar{V}_{ex}^{(2)}$ is found to be independent of φ_{3min} in this range, and to decrease from ~9 to ~3.4 Kcal/mole between 146°C and 194.5°C.

(iii) $\Delta\bar{V}_{ex}^{(3)}$ is found to be strongly dependent of φ_{3min}, with minima around $\varphi_{3min} = 90°$ for all temperatures. For fixed φ_{3min}, $\Delta\bar{V}_{ex}^{(3)}$ decreases with temperature in the range 146 to 194.5°C, whatever φ_{3min}.

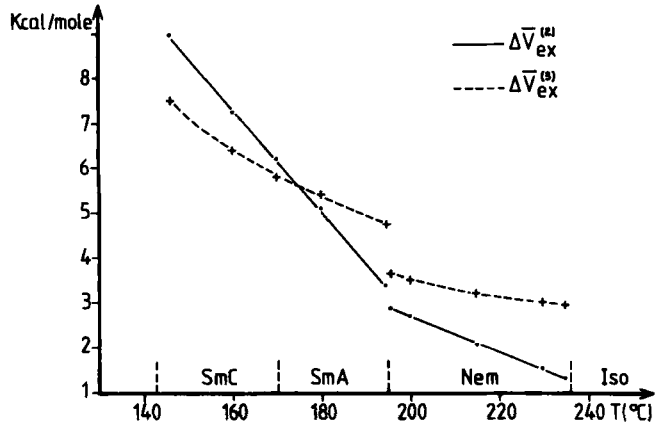

FIGURE 9 Temperature variation of the full heights $\Delta\bar{V}_{ex}^{(2)}$ and $\Delta\bar{V}_{ex}^{(3)}$ of the mean intermolecular potentials $\bar{V}_{ex}(\varphi_2)$ and $\bar{V}_{ex}(\varphi_3)$ assuming $\varphi_{3min} = 90°$. See section 6 for details.

(iv) φ_{2min} is found to be practically independent of φ_{3min} and equal to $\approx$116.5° within less than 0.5° between 146 and 194.5°C.

If we reasonably assume that $\Delta\bar{V}_{ex}^{(3)}$ should not be larger ~9 Kcal/mole, it is seen that in practice, the only physically possible situation is that corresponding to $\varphi_{2min} \approx 116.5°$, $\varphi_{3min} \approx 90°$, and $\Delta\bar{V}_{ex}^{(2)}$ and $\Delta\bar{V}_{ex}^{(3)}$ varying with temperature as shown in Figure 9, that we have deduced in detail from the calculation by fixing $\varphi_{3min} = 90°$.

If we consider now the combination of signs [−,+,−], the situation is completely different, although mathematical solutions can be found: φ_{2min} and φ_{3min} should be assumed to vary significantly with temperature, and the minimum possible value of $\Delta\bar{V}_{ex}^{(2)}$ at 146°C is 32 Kcal/mole, a situation which is clearly not realistic.

6b. The nematic phase

Although the problem of the signs of the R_{i1} has been solved from the analysis in the smectic phases, an uncertainty remains in the nematic phase concerning the assignment of the DMR splittings to the second and third methylene groups, since now we have $|\Delta\nu_2| \neq |\Delta\nu_3|$ (cf. Figure 4 and 5). The two possibilities are $|\Delta\nu_2|$ (resp. $|R_{21}|$) larger or smaller than $|\Delta\nu_3|$ (resp. $|R_{31}|$). We have tried the same kind of analysis as above for these two possibilities. We find that only the situation $|R_{21}| > |R_{31}|$ is reasonable since it predicts a decrease of $\Delta\bar{V}_{ex}^{(3)}$ at the smectic A–nematic transition, while the reverse situation predicts an increase of $\Delta\bar{V}_{ex}^{(3)}$ (cf. Figure 8b). Assuming $|R_{21}| > R_{31}$ we have com-

pleted Figure 8a,b,c for several temperatures in the nematic phase. Again the results are consistent with a situation where $\varphi_{3min} = 90°$ and φ_{2min} slightly varying with temperature from 116.5° to 119.5° i.e. no more than 3°. The corresponding $\Delta\bar{V}_{ex}^{(2)}$ and $\Delta\bar{V}_{ex}^{(3)}$ are shown in Figure 9. It is seen that these two quantities suffer discontinuities at the SmA–nematic transition and continue to decrease as the temperature increases.

6c. Discussion

The most remarkable result of this analysis are the features found for the intermolecular potentials $\bar{V}_{ex}(\varphi_2)$ and $\bar{V}_{ex}(\varphi_3)$. These features are precisely those which are physically expected (i) φ_{2min} and φ_{3min} are independent of temperature. This reflects the fact that at the molecular level, the geometry of the molecular surrounding is practically the same in all phases (e.g. the molecules are constrained to confine in a "cylinder" and (ii) the heights $\Delta\bar{V}_{ex}^{(2)}$ and $\Delta\bar{V}_{ex}^{(3)}$ decrease with temperature. This reflects a reduction of the constraints, or in other words, an increase of the free volume per molecule.

In Figure 10a,b, we have shown the shapes of $\bar{V}_{ex}(\varphi_2)$ and $\bar{V}_{ex}(\varphi_3)$ and in Figure 11a,b the shapes of the total potential $\bar{V}(\varphi_2)$ and $\bar{V}(\varphi_3)$,

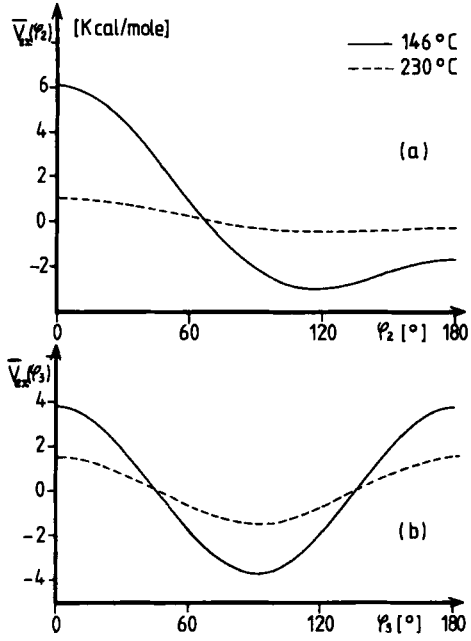

FIGURE 10 Shape of the mean intermolecular potentials for the two extreme temperatures 146°C and 230°C assuming $\varphi_{3min} = 90°$. a) $\bar{V}_{ex}(\varphi_2)$; b) $\bar{V}_{ex}(\varphi_3)$.

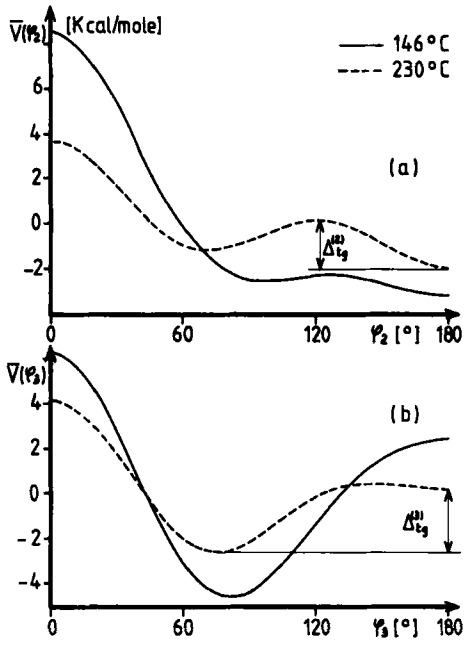

FIGURE 11 Shape of the mean total potentials for the two extreme temperatures, 146 and 230°C, assuming $\varphi_{3min} = 90°$. a) $\bar{V}(\varphi_2) = \bar{V}_{in}(\varphi_2) + \bar{V}_{ex}(\varphi_2)$; b) $\bar{V}(\varphi_3) = \bar{V}_{in}(\varphi_2) + \bar{V}_{ex}(\varphi_3)$.

for 146 and 230°C. Concerning the $\bar{V}_{ex}$, it is seen that they are minimum for values of the angles which are completely different from those in the isolated molecules (cf. Figure 6b,c). In particular $\bar{V}_{ex}(\varphi_2)$ is minimum at $\varphi_{2min} \sim 115$–$120°$, i.e. practically where $\bar{V}_{in}(\varphi_2)$ is maximum, between the trans and gauche positions. For the total potential $\bar{V}(\varphi_2)$, the effect of this is to smear out significantly the barrier between these two positions as can be observed on Figure 11a, this effect being more important at low temperature. This means that the rotation around the C_1C_2 bond between ~60 and 270° is easier in the liquid crystal than for the isolated molecule. Only the jump through $\varphi_2 = 0$ is more difficult. This is expected since $\varphi_2 = 0$ corresponds to a chain making a large angle with respect to the long molecular axis.

Concerning $\bar{V}_{ex}(\varphi_3)$, its shape is significantly different. The minimum is now at 90°, i.e. that the shape is practically a pure cos $2\varphi_3$. This means the liquid crystal medium tends to orient the $C_2C_3C_4$ plane perpendicular to the $C_1C_2C_3$ plane.

Figure 12a,b sketches the most probable conformations of the butyl chains imposed by the $\bar{V}_{in}$ (the all-trans) and the $\bar{V}_{ex}$ potentials, respec-

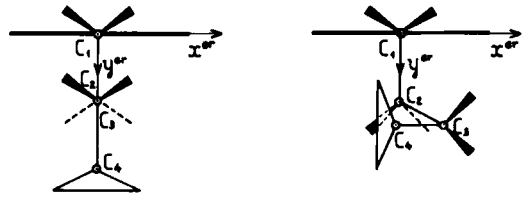

FIGURE 12 Sketch of the view, along the para-axis of the ring, of the most probable conformations of the butyl chains a) imposed by the intramolecular potentials: the all-trans conformation b) imposed by the intermolecular potentials. The most probable conformation in the liquid crystal is intermediate between a) and b) and changes with temperature.

tively. It is seen that conformation *b* is roughly speaking more confined in a cylinder containing the ring, as expected. The most probable conformation of the real chain is intermediate, between *a* and *b*, and determined by the relative amplitude of $\bar{V}_{in}$ and $\bar{V}_{ex}$. It is seen that the positions of the corresponding minima change slightly with temperature, as it is also the case for the aromatic core of TBBA.[14]

It is interesting to discuss the heights found for these various potentials in more detail. First the $\bar{V}_{in}$ correspond to about 4 Kcal/mole while the $\bar{V}_{ex}$ change from 8–9 to 1.5–3 Kcal/mole, according to the phase and the temperature. Being of the same order of magnitude, the details of the chain dynamics depend strongly of the precise physical situation, namely which phase and which temperature. The fact that the smectic A–nematic transition occurs when the $\bar{V}_{ex}$ becomes practically equal to the corresponding $\bar{V}_{in}$ is noticeable, but it is not clear for us if this result is fortuitous or contains some physical implications. Other details are of interest. Concerning the total potential $\bar{V}(\varphi_2)$, it seems that we can still define a (stable) trans position ($\varphi_2 = 180°$) and a gauche position situated between 90° and 70° according to the temperature. In Figure 13 we have plotted the barrier $\Delta_{tg}^{(2)}$ which separates these two positions. As stated above, it is seen that, at least in the smectic phases, this barrier is smaller than the corresponding one for the isolated molecule: $\Delta_{tg}^{(2)}{}_{in}$, showing that the rotation around C_1C_2 is more free between these two positions, as the medium becomes more dense. This apparently strange situation is easy to understand in terms of the above analysis. Concerning $\bar{V}(\varphi_3)$, the most stable position is always the gauche position whatever the temperature. This is illustrated in Figure 13 where we have represented the energy difference $\Delta_{tg}^{(3)}$ between the corresponding gauche and trans positions.

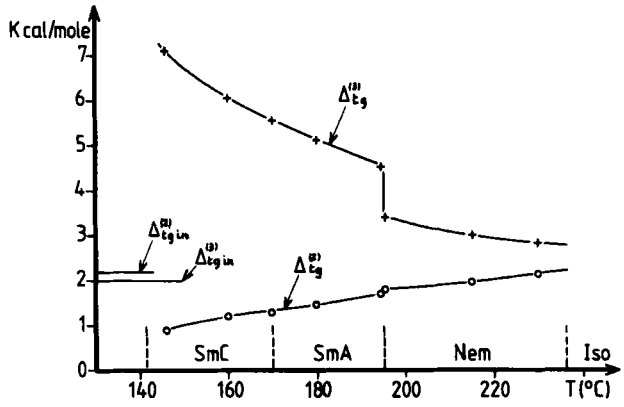

FIGURE 13 Temperature variation of the barrier heights Δ_{tg} between the trans and gauche positions for the second and third bonds C_1C_2 and C_2C_3. a) $\Delta_{tg}^{(2)}$ for C_1C_2 as defined in Figure 11a for 230°C. b) $\Delta_{tg}^{(3)}$ for C_2C_3 as defined in Figure 11b for 230°C. The corresponding heights $\Delta_{tg_{in}}^{(2)}$ and $\Delta_{tg_{in}}^{(3)}$ as defined in Figures 6b and 6c are also indicated.

7. SUMMARY AND CONCLUDING REMARKS

In summary, we have presented in this paper a simple model to explain quantitatively both the values and the temperature dependence of the DMR splittings associated with the butyl chains of TBBA, in the smectic C, smectic A and nematic phases, in terms of the intermolecular contribution to the potentials which hinder the rotations around the various C—C single bonds. We have determined both the shapes and the strengths of these potentials, which are well consistent with what is physically expected: the local geometry is practically the same in all phases and the free volume increases with temperature, with a discontinuity at the smectic A–nematic transition.[27] Due to the (necessary) approximations which have been made (decoupling hypothesis, representation of the $\bar{V}_{ex}$ by only two terms of their Fourier expansion, choice of $\varphi_{3min} = 90°$, experimental uncertainties), the various curves giving the shapes of the $\bar{V}_{ex}$ and of the $\bar{V}$, the values of the various barrier heights should be considered as semi-quantitative results only. However we are confident that they reflect satisfactorily the physical situation.

It should be said here that this work concerning the chains of TBBA is a natural continuation of the works presented in Refs. [15] and [14], where we were interested first in a description of the behavior of the molecule as a whole (external motions),[15] and then to the behavior of

the aromatic core (internal motions).[14] We emphasize here that we have chosen to describe the external motions in terms of the *single* order parameter $S_{z_0z_0}$, as a consequence of the analysis made in Ref. [15] of the ^{14}N NQR data published by the Llubjana group,[28] which convinced us that the second order parameter $S_{x_0x_0} - S_{y_0y_0}$, if not strictly zero, is too small to explain the observed temperature dependence of the DMR splittings in TBBA.[7,14]

It is also interesting to comment on the approach of other authors to similar data where the description of the chain ordering is based on the rotameric state model of Flory.[9,13] This model, which corresponds to rotational jumps between $\varphi = 180°$ and $\pm 60°$ around the C—C bonds in the isolated chain is modified by only changing the probabilities of occurrence of the various rotameric states, to take into account the influence of the medium. In terms of our mean potentials $\bar{V}$, this means that the $\bar{V}_{in}$ are modified in such a way that only the energy difference between the trans and gauche states changes. Since the shapes we found for the $\bar{V}$ are very different from those of the $\bar{V}_{in}$ (compare Figures 6 and 11), it is not surprising that this model cannot account quantitatively for the experimental data.

Acknowledgments

We are indebted to Dr. B. Deloche for kindly providing unpublished DMR data concerning the first methylene group of TBBA. Thanks also to Prof. A. Skoulios for illuminating discussions.

References

1. S. Marcelja, *J. Chem. Phys.*, **60**, 3599 (1974).
2. D. A. Pink, *J. Chem. Phys.*, **63**, 2533 (1975).
3. N. Boden, R. J. Bushby and C. D. Clark, *Chem. Phys. Lett.*, **64**, 519 (1979).
4. B. Deloche, J. Charvolin, L. Liebert and L. Strzelecki, *J. Physique Colloques*, **36**, C1-21 (1975).
5. P. J. Bos and J. W. Doane, *Phys. Rev. Lett.*, **40**, 1030 (1978).
6. A. F. Martins, *Phys. Rev. Lett.*, **44**, 158 (1980).
7. F. Volino and A. J. Dianoux, *Mol. Cryst. Liq. Cryst. Lett.*, **49**, 153 (1979).
8. B. Deloche and J. Charvolin, *J. Phys. Lett.*, **41**, L39 (1980).
9. S. Hsi, H. Zimmermann and Z. Luz, *J. Chem. Phys.*, **69**, 4126 (1978).
10. N. Boden, L. D. Clark, R. J. Bushby, J. W. Emsley, G. R. Luckhurst and C. P. Stockley, *Mol. Phys.*, **42**, 565 (1981).
11. N. Boden, R. J. Bushby and L. D. Clark, *Mol. Phys.*, **38**, 1683 (1979).
12. P. J. Flory, *Statistical Mechanics of Chain Molecules*, Interscience N.Y. (1969).
13. J. W. Emsley, G. R. Luckhurst and C. P. Stockley, *Mol. Phys.*, **38**, 1687 (1979).
14. A. J. Dianoux and F. Volino, *J. Physique*, **41**, 1147 (1980).
15. A. J. Dianoux and F. Volino, *J. Physique*, **40**, 181 (1979).
16. J. Charvolin and B. Deloche, *J. Physique Coll.*, **37**, C3-69 (1976).

17. Z. Luz, R. C. Hewitt and S. Meiboom, *J. Chem. Phys.*, **61**, 1758 (1974).
18. F. Volino, A. F. Martins and A. J. Dianoux, *Mol. Cryst. Liq. Cryst.*, **66**, 37 (1981).
19. D. M. Brink and G. R. Satchler, "Angular Momentum" (O.U.P.) p. 24 (1968).
20. This non equivalence has recently been observed for a methylene group in the lateral chain of poly (γ-benzyl.L. glutamate): PBLG, a chiral lyotropic liquid crystal polymer (K. Czarniecka and E. T. Samulski, *Mol. Cryst. Liq. Cryst.*, **70**, 205 (1981).
21. The unpublished data concerning $|\Delta\nu_1|$ was kindly provided by Dr. B. Deloche.
22. J. Bergès and H. Perrin in "Liquid crystals of one and two dimensional order," Eds. W. Helfrich and G. Heppke, Springer-Verlag (1980) pp. 77 and 89.
23. H. Perrin and J. Bergès, *J. Physique Lettres*, **43**, L531 (1982).
24. J. Doucet, J. P. Mornon, R. Chevalier and A. Lifchitz, *Acta Crystallogr.*, **B33**, 1701 (1977).
25. M. V. Volkenstein in "Configurational Statistics of Polymeric Chains," High Polymers Gl. XVII, Interscience p. 104 (1963).
26. A. J. Hopfinger in "Conformational Properties of Macromolecules," Academic Press p. 4 (1973).
27. Molar volume data concerning the solid and the various smectic phases of TBBA (but not the nematic phase) are published in "D. Guillon and A. Skoulios, *J. Physique*, **38**, 79 (1977)."
28. J. Seliger, V. Žagar and R. Blinc, *Phys. Rev.*, **A17**, 1149 (1978).